(CERN) SI/Int. DL/68-5
11.12.1968

THE 800 MEV SPECTROMETER FOR THE BOOSTER

POSSIBLE SOLUTIONS

C. Bovet and H. Koziol

SI/Int. DL/68-5
11.12.1968

THE 800 MEV SPECTROMETER FOR THE BOOSTER

POSSIBLE SOLUTIONS

C. Bovet and H. Koziol

E R R A T A

P. 10, last equation : read correctly $\frac{\Delta s \ \hat{x}'^2}{2} = \frac{5}{100} 4 \varepsilon_s$

P. 11, first equation: read correctly $\Delta x = \sqrt{2.5 \ \varepsilon_s \Delta s}$

P. 19, 10th line from top : read "detector plane" instead of "detector"

Fig. 1 : read "$+10^o$" instead of "-10^o"

Fig. 5a : the dotted ellipse is missing;

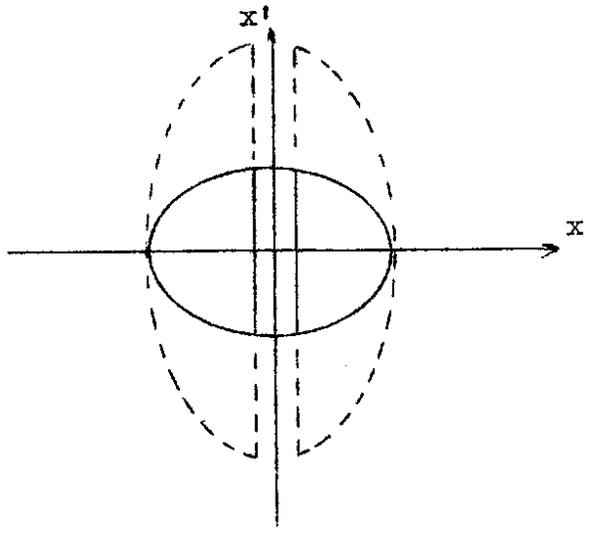

Fig. 6, left vert. coord. : read "F_B" instead of "B".

NOTATIONS

1. We will use the following co-ordinate system:

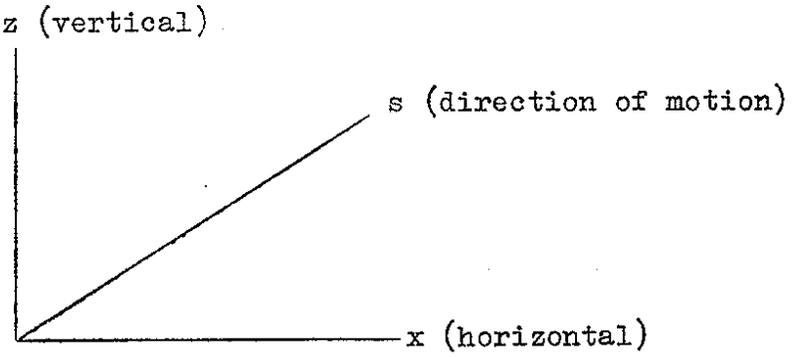

2. The emittance of a beam is:

$$\varepsilon = \frac{\text{area of ellipse}}{\pi}$$

3. Widths of distribution ($\Delta E, \Delta p$) are always total widths, e.g. ΔE = 2.50 MeV and not $\pm$ 1.25 MeV

4. Δ refers to widths or differences within one beam
δ refers to differences between two beams.

I. INTRODUCTION

During any operation of the Booster without injection into the PS (a situation which one will have in particular during the running-in period and later on with all machine experiments not involving the PS), the protons, accelerated in the Booster to 800 MeV, will have to be dumped in a safe place.

For this purpose the beams will be ejected in the usual way from the four rings into the transfer line. Somewhat downstream of the point of full recombination (i.e. transfer kicker magnet KM3) and before the transfer line passes through the wall to the PS, a bending magnet will deflect the beams into a "beam dump", which consists of a 5 m deep hole into the earth, about 18 m from the transfer line at the end of the "spectrometer hall" (Fig. 1).

It has been suggested in 1967 by K.H. Reich, to make use of this bending magnet and to perform some kind of momentum analysis of the ejected beams. This could yield valuable information for the running-in and for later machine experiments.

It is of considerable interest to know the momentum distribution of the protons in the four beams of the Booster and to investigate its dependance, e.g. on the RF-gymnastics during acceleration. Information on this can be gained from measurements of the longitudinal density distribution of the beams and comparison with the bucket shapes, also by trapping experiments in the PS. But a more direct measurement would certainly be welcome.

Our first approach was therefore to design a spectrometer which would allow one to investigate the momentum distribution $\frac{dn}{dp}(p)$ of the protons in each of the four sequentially ejected beams. We will call this design the "real spectrometer".

According to ref [1] the total width of the momentum distribution at the moment of ejection is

$$\left(\frac{\Delta p}{p}\right)_{beam} \approx 2.10^{-3}$$

and for a reasonable analysis one has to ask for a resolution of at least 1/10 of this value and if possible better. The value assumed for the design of the real spectrometer was

$$\left(\frac{\Delta p}{p}\right)_{res} = 1\ 10^{-4}\ .$$

As shown in II. it may be feasible to obtain this resolution, perhaps not right from the start, but after some time of operation to find out the necessary final touches.

This solution, however, requires a separate 30° spectrometer magnet of large aperture and high precision and several additional quadrupoles lenses, also of large aperture and high precision, not to forget the power supplies, that go with them. The effort, both in development and in money, is substantial.

Therefore we looked into the possibility of contenting oneself with a simpler and consequently less expensive spectrometer with limited performance. We will call this version the "restricted spectrometer".

It will still allow one to compare the average momenta of the 20 sequentially ejected bunches with a precision of

$$\left(\frac{\delta \bar{p}}{\bar{p}}\right)_{res} = 1\ 10^{-4}$$

but without giving information on the momentum distribution. This resolution has to be compared (see V.) with the value of $\delta\overline{p}/\overline{p}$ which one can expect for a properly functioning Booster.

In the following chapters we will briefly discuss the principles and the technical consequences of both versions and give a rough comparison of costs.

It is hoped that, on the basis of this report, a choice between the two proposed versions can be made.

For either version one can install additional detectors in the spectrometer line to measure the emittance of the ejected beams or, at least, to indicate changes.

II. REAL SPECTROMETER

As any proper image spectrometer it will consist of a slit, a few lenses to image the slit onto a detector and a bending magnet to introduce the dispersion.

It has been said that the required momentum resolution is

$$\left(\frac{\Delta p}{p_o}\right)_{res} = 1.10^{-4} \quad . \qquad (1)$$

The resolution can best be discussed in terms of the emittance ellipses at the exit of the bending magnet (see Fig. 2).

All particles with the central momentum $p = p_o$ will be contained in an emittance ellipse, which has its centre at the origin of the (x,x')-plane. For particles with a different momentum $p = p_o + \Delta p$ the centre of their emittance ellipse will be shifted by $\Delta x'$. With φ as the bending

angle of the magnet

$$\Delta x' = \varphi \cdot \frac{\Delta p}{p_o} \quad . \qquad (2)^{*)}$$

Ellipses which do not overlap in the (x,x')-plane can be transformed into ellipses which are completely separated in x at $s = s$ (detector). Therefore the smallest Δp which can be resolved, is that which displaces the centre of the ellipse by $(\Delta x')_{res} = 2x_o'$ **). Consequently

$$\left(\frac{\Delta p}{p_o}\right)_{res} = \frac{2x_o'}{\varphi} \qquad (3)$$

Since $\varepsilon = \hat{x}\, x_o'$

$$\left(\frac{\Delta p}{p_o}\right)_{res} = \frac{2\varepsilon}{\hat{x}\varphi} \qquad (4)$$

It follows that to obtain a high resolution one has to meet the following requirements:

1. A large bending angle φ.

   The limit will be given by cost and space considerations.

2. A small emittance ε

   This is obtained by reducing the emittance of the original beam by means of a slit.
   Limiting factors are intensity considerations for the detector and scattering effects at the slit.

3. A large beam width $2\hat{x}$ in the bending magnet

   A wide beam is obtained with the help of quadrupole lenses.
   Limiting factors are quality and cost considerations for the large aperture lenses and bending magnet.

---

*) Correctly, φ should be replaced by $2\sin \varphi/2$ for a sector magnet and by $2\,\mathrm{tg}\, \varphi/2$ for a rectangular magnet. For $\varphi = 30^o$ eq. (2) is correct to $2^o/o$.

**) One could give a less stringent condition for resolution: assuming e.g. a Gaussian density distribution, it is sufficient to separate the ellipses in x' by twice the half width of $\frac{dn}{dx'}(x')$.

The "classical" arrangement of a spectrometer is shown in Fig. 3 together with a typical evolution of the emittance ellipse. In our case the elements upstream of the bending magnet cannot be arranged in this straight forward way, but have to be filled in-between the elements of the transfer line such as not to prejudice in any way the transfer from the Booster to the PS.

We shall now discuss the elements of the spectrometer in a sequence, which leads in the most logical way to the determination of the parameters:

bending magnet
emittance of sample beam
slit
detectors
general layout.

The bending magnet

It being the biggest item influencing strongest the general layout, its main parameters were determined first.

The fact that a high quality, large aperture magnet was required, led away from the original layout indicated in Fig. 1. High quality means not too high fields and this together with a wide beam would lead to an enormous aperture (not less than 1 m at 10 kG, with $+ 10^{\circ}$, $- 24^{\circ}$, $\ell \approx 2$ m).

As a consequence the original two way magnet was replaced by two one way magnets (Fig. 4). The first one is shifted upstream of the original position by 1.5 m and bends the beam into the transfer line to the PS by $\approx 9^{\circ}$. It can be a relatively low quality, high field and therefore short magnet ($\ell \approx 0.54$ m at 15 kG). It is switched off when the beam is directed to the beam dump, but its aperture has to be sufficiently large (about 0.4 m) to pass the wide spectrometer beam.

The spectrometer magnet has to be so far downstream of the first bending magnet that it clears the transfer line. To keep this distance within the limits of the building and looking for good field quality, a C-type, window frame magnet has been chosen, with the yoke on the inside of the curvature. The required clearance together with the gap and coil width and the field strength of 10 kG determine the position of the entrance of the magnet and of the centre of curvature. To save aperture a sector shape has been chosen.

To gain in resolution and to have the detectors at a convenient distance from the wall the bending angle is increased from 24° to $\varphi=30^{\circ}$.

For the horizontal aperture there is the argument that one wants a beam as wide as possible in the magnet and we have assumed that it is reasonable to ask for a good field region over $2\hat{x} = 0.2$ m. The total aperture has to be considerably wider. As discussed later, the total beam will suffer an emittance blow-up by 64 °/o due to scattering on the slit material. A total free gap width of 0.4 m will be about adequate. The gap height will have to be 0.15 m (this is given by the vertical envelope).

To sum up the parameters:

configuration	sector magnet C-type, yoke on the inside window frame coils
free aperture	hor. : 0.4 m vert.: 0.15 m
field strength	10 kG
bending radius	$\rho = 4.881$ m
bending angle	$\varphi = 30^{\circ} = 0.5236$ rad
length along s	$\ell = 2.556$ m.

We can now take eq. (4) and calculate the maximum emittance we can allow for the spectrometer beam

$$1\ 10^{-4} = \frac{2\,\varepsilon}{0.1\text{m}\ 0.5236\ \text{rad}} \qquad (4')$$

$$\varepsilon_s = 2.62\ \text{mm mrad} \qquad (5)$$

which means that, with a horizontal emittance of the total ejected beam of $\varepsilon_t = 33$ mm mrad, nearly all of the beam (87°/o, assuming a gaussian density distribution) has to be done away with. This leads us to the next item.

The slit

A slit is usually a device which is brought into a beam to stop all particles outside a certain range $x_o \pm \Delta x$, in order to obtain a source of particles with well defined position and size. This is also required in our case, but we cannot afford to stop the protons for the following reasons:

1. To stop 10^{13} protons per second at 800 MeV would create intolerably high radiation levels. After all, the primary purpose of the spectrometer is to bring the protons to the beam dump!

2. Even with platinum as material for the slit, the range of 800 MeV protons is 21 cm (lead: 40 cm). The slit, having a width of a fraction of a millimeter would therefore limit the beam not only in x, but also strongly in x'.

3. With such an extension in the s-direction a considerable fraction of the protons entering the slit will leave it and transverse part of the length of the jaw material, thus increasing the effective width of the slit and adding a low energy tail to the original energy distribution.

A solution is to make the jaws of the slit only so thick, that the protons incident on them are not stopped but only degraded in energy to such an extent, that they are imaged in the detector plane sufficiently far away from the image of the slit. Considering

1. the width of the energy distribution of the protons of $\Delta E = 2.5$ MeV.

2. the additional energy distribution which the degraded protons suffer from the "straggling" in the material of the jaws,

3. the size of the degraded beam in relation to the dispersion dx/dp at the detector,

one arrives at a required degrading of

$$(\Delta E)_{deg} = 10 \text{ MeV} . \qquad (6)$$

For protons traversing such a degrading material one has to consider the following effects:

energy loss
straggling
scattering
nuclear interactions.

Energy loss. Particles traversing matter will loose energy by exciting or ionizing the atoms along their path. The energy loss can be calculated by the Bethe-formula (ref. 2, p. 440, in the gaussian system of units):

$$\frac{dE}{ds} = 4\pi N Z \frac{z^2 e^4}{m_o \beta^2 c^2} \left[\ln \left(\frac{2\gamma^2 m_o \beta^2 c^2}{\hbar < \omega >} \right) - \beta^2 \right] \qquad (7)$$

N	Avogadro's number (atoms/cm^3)
Z	atomic number
ze	charge of particle
m_o	electron rest mass
$\langle\omega\rangle$	mean of harmonic binding frequency
γ,β	relativistic parameters of particle

Numerical values of dE/ds, calculated with corrections for the inner electron shells, are tabulated in [3] of which a few values are given in Table I.

Straggling. As the protons loose their energy in discrete amounts in statistically occuring events, the losses for the individual protons will be distributed around the mean value as given by eq. (7). An originally monochromatic beam will leave the slice of matter with a Gaussian energy distribution. The rms-value $\langle\Delta E\rangle$ of this distribution, calculated according to [4], is given in Table I, also in terms of $\Delta p/p$. If the original beam already had an energy distribution, the two distributions have to be added adequately.

Scattering. Apart from the inelastic interactions with the electrons, the protons will also undergo Coulomb scattering by the nuclei, leading to an angular deflection of the protons. The rms-value of the total deflection the protons will suffer after traversing a slice of matter of thickness Δs, can be calculated according to ref. 2, p. 456:

$$\langle\theta\rangle = \frac{2z\,Z\,e^2}{p\beta c}\left[2\pi N \ln\left(\frac{\theta_{max}}{\theta_{min}}\right)\Delta s\right]^{1/2} \qquad (8)$$

θ_{max}, θ_{min}: cut-off angles of the scattering cross section.

For our purpose we have to consider the projections of all angles θ onto one transverse plane:

$$\langle\theta\rangle_{proj} = \frac{1}{\sqrt{2}}\langle\theta\rangle .$$

Numerical values are given in Table I.

Nuclear interactions. A fraction of the protons traversing the jaws of the slit will undergo inelastic interactions with the nuclei of the material and are consequently lost from the beam. The probability for such an interaction over a certain pathlength can be calculated from the cross-section for such processes. The values calculated for Table I are based on the data given in [3].

The slit width $2\Delta x$ may be found by the following argumentation:

Fig. 5a shows how the slit outs the sample beam from the total beam. In Fig. 5b the sample beam is shown as it enters and as it leaves the slit of length Δs. The protons in the horizontally shaded areas have entered the slit at its entrance, but left it later on and traversed part of the jaws. The protons in the vertically shaded areas on the other hand have traversed part of the jaws before entering the slit. Fig. 5c indicates the four possibilities for the protons. The protons in the hexagonal unshaded area are completely undegraded, the protons in the shaded areas have lost between 0 and 10 MeV. We consider it a tolerable disturbance of the original energy distribution of the sample beam if of all the partially degraded protons 5°/o fall within the distribution width of 2.5 MeV. This means that 2.5/10 of the shaded area shall correspond to not more than 5°/o of the total area.

Total area : $4\ \Delta x\ \hat{x}' = 4\ \varepsilon_s = 4\ 2.62\ 10^{-6}$ m rad *)

Shaded area : $2\ \Delta s\ \hat{x}'^2$

$$\frac{\Delta s\ \hat{x}'^2}{2} = \frac{5}{100}\ \varepsilon_s$$

*) Under the given circumstances i.e. ellipse in principal position at the slit and inside the magnet one should take the inscribed ellipse as representative for the rectangular sample.

with $\hat{x}' = \varepsilon_s/\Delta x$ we obtain

$$\Delta x = \sqrt{10\ \varepsilon_s\ \Delta s}$$

and with the value for ε_s and converting to millimeters

$$\Delta x = 0.0809\ \sqrt{\Delta s} \qquad (9)$$

$\Delta x, \Delta s$ in mm.

The values of $2\Delta x$ are also listed in Table I as well as the value $\hat{x}'$ which results for the incoming and therefore also for the sample beam from the given Δx and $\varepsilon = 2.62$ mm mrad.

Due to the scattering in the jaws the emittance of the total beam will increase. This is indicated by the dotted ellipse in Fig. 5a. The $\hat{x}'^*$ of the total beam after scattering has been calculated under the assumption that the beam density distribution is Gaussian in the phase plane (x,x') and that the envelope is taken at 2σ (i.e. it includes 95°/o of all protons). The scattering having also a Gaussian distribution which is added onto the original one, one obtains the $\hat{x}'^*$, after scattering by

$$\hat{x}'^* = 2\left[\left(\frac{\hat{x}'}{2}\right)^2 + \langle\theta\rangle^2_{proj}\right]^{1/2}. \qquad (10)$$

The ratio $\hat{x}'^*/\hat{x}' = \varepsilon^*/\varepsilon = F_B$, which constitutes a blow-up factor, is also given in Table I. The width of the total beam inside the bending magnet and the adjacent lenses will be wider by this factor than the sample beam and this determines the necessary aperture with all its technical and financial consequences.

At first sight beryllium seems to be the obvious choice as material for the jaws, as it gives the least blow-up for a degrading by 10 MeV. However, with an $\hat{x}' = 6.0$ mrad unreasonably high gradients would be required in the following two lenses, to make an $\hat{x} = 100$ mm wide and parallel beam inside the spectrometer magnet, their position and maximum length being restricted by the elements of the transfer line. In order to obtain a bigger permitted $\hat{x}'$ one has to choose a material with a bigger dE/ds which inevitably brings with it a bigger blow-up factor for the scattered total beam.

In order to find a reasonable compromise, the blow-up factor F_B and the maximum permitted $\hat{x}'$, under the above discussed conditions, has been calculated for a large number of materials which can be considered from the technological point of view and for which sufficient data could be found. The results are plotted in Fig. 6 as a function of the atomic number Z.

It is a very fortunate coincidence that for nickel (Z = 28) one finds at the same time a relative maximum of $\hat{x}'$ and a relative minimum of F_B.

An $F_B = 1.64$ may appear very high, but it is already 1.43 for beryllium and, as we will see later, the requirements on the quality of field in the lenses and in the bending magnet are such that the sample beam can only occupy at maximum 2/3 of the apertures. The total beam may make use of the lower quality field regions.

Nickel has therefore been adopted as material for the jaws of the slit.

The detector

With a dispersion in the detector plane of 7.5 mm/MeV the sample beam, having 2.5 MeV of total energy spread, will be about 19 mm wide. This

width has to be divided into at least 20 channels, so that a spatial resolution of 0.9 mm is required. It is proposed to use an arrangement of thin wires, as described in [5], which collect charge by secondary emission. The signals will be amplified by cathode followers situated very close by. The situation at the detector is illustrated in Fig. 11a.

The ejection from the Booster being arranged such that the beams from the four rings are ejected head to tail of each other, the signals will have to be gated after each 5 bunches, i.e. every 620 nsec, into four different channels, as one wants to investigate the energy distribution for each of the four rings separately. The change over time may be about 50 nsec. The electronics for the intermediate signal storage and the channel scanning has at this stage not yet been looked into.

The following estimate on the signal levels to be expected can be made:

nominal number of protons per ring	$2.5\ 10^{12}$
running at 10 °/o of nominal intensity	0.1
sample beam/total beam (Gaussian distribution)	0.13
with a Gaussian distribution and 20 channels the outmost wires will receive 1.3 °/o of the total sample beam	0.013
secondary emission coefficient	0.03

This means that under the above given conditions a charge of $1.3\ 10^{7}$ e = $2.1\ 10^{-12}$ C will be collected. Assuming a capacity of $\approx$ 100 pF from the wire to the cathode follower, this constitutes a signal of $\approx$ 20 mV. This calls for a noise level inferior to $\approx$ 5 mV.

General layout

A first proposal for the arrangement of the lenses has been made by A. Ball [6]. The development since then of the design and the

fixing of the parameters discussed until now have,led us to the layout shown in Fig. 4. The shaded elements have been added to the elements of the transfer line. The horizontal and vertical beam envelopes are shown in Fig. 7. The horizontal envelope is drawn for the sample beam, for the total beam it is larger by 1.64 inside the bending magnet. The vertical envelope is drawn for an emittance fo 35 mm mrad, i.e. for ejection in the "10-bunch mode", for which the beams also have to be brought safely to the beam dump. The vertical amplitudes for the 10-bunch mode and for the normal 20-bunch mode,but with scattering at the jaws,are practically the same.

The slit is arranged as far upstream as possible, but still downstream of the kicker magnet KM3, as about 4°/o of all the protons will undergo nuclear interactions in the jaws of the slit.

The doublet Q_{s1} and Q_{s2} creates the proper conditions at the slit, i.e. the correct $\hat{x}'$ for the sample beam and a large $\hat{z}'$ to minimize the scattering effect also in the vertical plane. This, however, is not easy to obtain and no solution has been established yet. $Q_{s3} = Q_4$ increases the horizontal divergence to bring the beam to the required $\hat{x}$ = 100 mm within the short distance available. Q_{s4} makes the beam parallel and the doublet Q_{s5} and Q_{s6} focuses the beam in both planes onto the detector. The required lens parameters are also given in Fig. 7.

Aberrations and quality requirements

So far all calculations have been based on the assumption of perfect elements and on paraxial optics. With the high resolution required it is indispensable to look into effects due to trajectories far from the axis and due to imperfections in the fields. This has been done in a report by C. Metzger [7], of which we will quote here the main results.

The image plane at the detector is not at 90° with the s-direction, but encloses with it an angle of $\psi = 7.5^{\circ}$ only, which creates certain difficulties for the detector. The values for ψ for similar spectrometers at DESY, SLAC, etc., are also of this order. Introduction of sextupole lenses can help very much to increase ψ (from originally $\approx 3^{\circ}$ to $\approx 45^{\circ}$ for the SLAC 20 GeV spectrometer, see [8]), but inevitably reduces the resolution strongly. So we would have to live with the 7.5°.

The quality required for the lenses is that $\frac{1}{r}\int Bds$ does not vary by more than $1\ 10^{-3}$ over the aperture occupied by the beam.

For the bending magnet it has tentatively been assumed that the value $\frac{1}{R}\int Bds$, measured along curves of different radii R, does not change by more than $1\ 10^{-4}$ over the aperture occupied by the sample beam.

If it would turn out, that to reduce the aberrations and the effects of the imperfections in the fields, one had to reduce the width of the sample beam, one could introduce a second slit downstream of the first one. This would reduce the width in the spectrometer magnet and the adjacent lenses, but also reduce the emittance and therefore the signals at the detector by the same amount. The total aperture of the magnetic elements would still have to be the same as with one slit only, to take the total blown-up beam. The two slits would degrade by 5 MeV each and three beams instead of two would arrive at the detector: of 800, 795 and 790 MeV.

III. RESTRICTED SPECTROMETER

The adjective "restricted" should indicate that this is not a proper spectrometer in the usual sense and that it gives only limited information. Whereas with the "real" spectrometer one obtains information about the energy distributions and their centre values for the

four beams ejected from the four rings, the "restricted" one will give information only on the centre values of energy for the four beams, i.e., one can measure only the differences $\delta\overline{E}$ or $\delta\overline{p}$ between the different beams. Probably the time resolution will even be good enough to obtain the individual $\delta\overline{p}$ for each of the 20 bunches.

As one does not want any more to resolve the energy distribution, the most stringent conditions appearing for the real spectrometer, i.e., very narrow slit, wide beam in the bending magnet, high precision magnet and lenses, become unnecessary.

The density distribution at the detector will no longer be given by the energy distribution of the protons, but by the distribution of their betatron amplitudes. However, the centre value of the density $\frac{dn}{dx}(x)$, whichever definition it may be given, will still be an unambiguous function of the average momentum of all the protons, and can easily be detected separately for the four beams or even for each of the 20 bunches.

The high quality requirement for the bending magnet being abandoned, one could return to the original layout of Fig. 1. But in order to avoid the very large aperture due to the sagittae for $+9/-24^{\circ}$, we considered it better to have also in this case two magnets (see Fig. 9). The first one is in the same position as for the real spectrometer, but is now arranged to bend by $\approx 10^{\circ}$ in both directions. The second one is so far downstream as to give sufficient clearance to the transfer line and its angle is the smallest one which can direct the beam to the end of the dump tube, arranged for the real spectrometer. The total bending angle of $\approx 26^{\circ}$ is only 1 to 2° more than that of Fig. 1.

We shall now discuss briefly the following aspects:

principle
target and detector
general layout.

Principle

Consider two beams with different average momenta, $\bar{p}$ and $\bar{p} + \delta\bar{p}$, with their centre lines as shown in Fig. 8a. The dispersion at the detector is roughly given by

$$\delta x = \varphi L \frac{\delta\bar{p}}{\bar{p}} . \qquad (11)$$

With $\varphi \approx 26^{\circ} \approx 450$ mrad and $L \approx 16$ m one obtains a $\delta x \approx 0.7$ mm for a $\delta\bar{p}/\bar{p} = 1\ 10^{-4}$, the resolution one is aiming at.

A displacement of this size is easily measured, even if the beam width $2\Delta x$ is considerably bigger than that, e.g. with a pair of thin plates using the secondary emission effect (Fig. 8b).

For a beam with rectangular density distribution in x the signals from the two plates being I_1 and I_2 we have

$$\frac{I_2 - I_1}{I_2 + I_1} = \frac{\Delta I}{I} = \frac{\delta x}{\Delta x} \qquad (12)$$

and for any real density distribution the ratios will be of the same order of magnitude.

Assuming a resolution in signal size of $\Delta I/I = 10^{-2}$ we get the maximum permissible beam size at the detector

$$\Delta x \leq 100\ \delta x . \qquad (13)$$

Transferring back to the bending magnet B (Fig. 8a) and using eq. (11) this means (see Fig. 8c)

$$x_o' \leq 100\ \delta x'$$

$$x_o' \leq 4.5 \text{ mrad} \quad \text{for } \delta\bar{p}/\bar{p} = 1\ 10^{-4} .$$

With ε = 33 mm mrad this gives us a minimum half-width of the beam in the bending magnet

$$\hat{x} = \frac{\varepsilon}{x_o'} \geq 7.3 \text{ mm}$$

which is fulfilled anyway.

Variations of the beam position at the detector will also occur for beams with equal $\bar{p}$ but coming down the transfer line along different trajectories. There are four possibilities to account for this:

1. One could place a split-plate detector, so thin as to have negligible scattering and degrading effects, at the place marked "target" in Fig. 9, measure the changes in position and correct the result at the final detector. This can be done by a simple addition of the two signals $\Delta I/I$ from the two detectors. At least the same accuracy is required for the monitoring detector as for the measuring one.

If one wants to avoid correcting in this way, then one has to create a sample beam coming from a slit or target with constant position:

2. Exactly the same arrangement as for the real spectrometer can be made, i.e. a slit with jaws degrading by 10 MeV will be put in the same place as shown in Fig. 4. Also here this would necessitate a doublet upstream of KM3 to focus in both planes onto the slit. The situation at the detector would be as shown in Fig. 11a, only that the wire detector would be replaced by a split-plate detector.

3. As the momentum distribution $\frac{dn}{dp}(p)$ is no longer of interest, we can permit it to be perturbed. Therefore the slit can be replaced by an "antislit", i.e. by a degrader $2\Delta x$ wide and Δs long. It is now the sample beam which is degraded. The situation will practically be as in Fig. 11a, only that the beams are now reversed in x and it is now the sample beam which is widened by the momentum straggling in the degrader. Beam optically it is the same as 1. The use of an antislit reduces the number of nuclear interactions by a factor ≈ 10.

4. Quite a different possibility is to separate the sample beam not by degrading and subsequent horizontal separation, but by scattering and subsequent vertical separation.
A thin vertical wire is put into the beam at a place where the conditions are such that the scattering has a great influence on the emittance in the vertical plane, but only a small one in the horizontal plane ($x_o' > z_o'$). Arranging the optics such that in the horizontal plane there is imaging onto the detector and that in the vertical plane the unscattered part of the beam is focussed onto the detector but not so the scattered part, the situation at the detector is as shown in Fig. 11b. With a $z_o' = 0.7$ mrad at the target, a 1 mm aluminium wire will blow up the σ of the vertical distribution by a factor of ≈ 3. 19°/o of the scattered particles can be detected outside the main beam on either side.

Versions 1 and 4 require no additional doublet upstream of KM3 which is difficult to realise anyway. They have therefore been chosen for the general layout.

General layout

It is shown in Fig. 9. The monitoring detector or the scattering wire target is put at a place with suitable conditions ($x_o' > z_o'$). The envelopes of Fig. 10 are calculated with the scattering being taken into account and include 95°/o of the sample beam. For case 1 the vertical envelope will be somewhat smaller.

$Q_{s1} = Q_4$ and Q_{s2} produce a rather parallel beam in both planes through the bending magnets, with an envelope much smaller than that for the real spectrometer. Q_{s3} and Q_{s4} focus onto the detector in the way described under case 4.

IV. COMPARISON OF COST

We do not intend to give a complete cost estimate for each version of spectrometer, but only a differential comparison of the costs for the magnet systems, including power supplies.

of voltage cannot be turned off sufficiently fast and for financial

The prices given in Tables II and III were estimated by P. Bossard and are for this purpose accurate to only 20°/o for each element. The total sums are

real spectrometer	870 kFr
restricted spectrometer	365 kFr
difference	505 kFr.

Not included are lenses used for the spectrometer but installed anyway for the transfer. Neither are included items which cost about the same for either version, as slits and vacuum system. The detector with all data transfer may however be cheaper for the restricted spectrometer by as much as 50 kFr.

It can therefore be concluded that the real spectrometer is more expensive than the restricted one by about 500 to 600 kFr, not counting the considerably higher effort in man power.

A design with no other purpose than to dump the beam would be little less expensive than the restricted spectrometer. All one would save is one lens with its power supply (15 kFr + 30 kFr), the slit or target (max 20 kFr), the detector with its electronics (50 kFr) and the mechanical devices for accurate alignment. The vacuum system (10 kFr) would have to be installed anyway. Altogether one might save only about 110 kFr.

In other words: the restricted spectrometer costs about 110 kFr above the bare minimum and the real spectrometer about 660 kFr.

V. CONCLUSIONS

We do not intend to make any choice between the two versions but just discuss their respective merits.

The real spectrometer is clearly the much more expensive version and would demand considerable further development. It cannot be guaranteed that it will work to specifications from the start and the ultimate shimming, trimming and tuning with the beam on may take quite some time.

There are three other possible means to obtain information on $\frac{dn}{dp}(p)$:

1. Observation of the longitudinal density distribution in the circulating beams. This presupposes exact knowledge of the bucket shape, including space charge effects.

2. Scanning with empty buckets of the coasting beams. This necessitates the facility for an abrupt turn-off of the accelerating rf or a second accelerating cavity to perform a rapid phase shift by π, followed by a normal turn-down of the voltage.

3. Trapping experiments in the PS.

Measurements 1 and 2 are possible at any energy between 50 and 800 MeV. 3 can be excluded for the running-in or any longer development runs. Measurement 2 will probably be not available, as the rf voltage cannot be turned off sufficiently fast and for financial reasons it is not foreseen to have a second cavity even in one ring.

How desirable the real spectrometer is, depends on how much weight one puts on the knowledge of the momentum distribution and how much confidence one has in measurement 1. To discuss these two questions is beyond the aim of this report.

The restricted spectrometer is not much more expensive than what is needed anyhow to bring the beam to the dump. No high precision elements are required and one can expect it to work properly practically from the start.

We have said, that the resolution in $\delta\bar{p}/\bar{p}$ will be $1\ 10^{-4}$ or possibly even $5\ 10^{-5}$. With a resolution of $1\ 10^{-4}$, the momentum spread of the protons being $\Delta p/p = 2\ 10^{-3}$, one can check the equality of the momenta of the 20 bunches to a degree which corresponds to a dilution of $10^{o}/o$ in the longitudinal phase plane, when they are trapped in the PS.

We may now ask what inequality of the momenta of the four beams of the Booster we may expect. Taking the equations of [9] and comparing any two rings:

$$\frac{\delta\bar{p}}{\bar{p}} = \frac{\gamma^2}{\gamma^2 - \gamma_{tr}^2}\,\frac{\delta\bar{B}}{\bar{B}} - \frac{\gamma^2\,\gamma_{tr}^2}{\gamma^2 - \gamma_{tr}^2}\,\frac{\delta\bar{f}}{\bar{f}}\,.$$

With $\gamma_{tr} \approx Q_H \approx 4.7$ and for $E_k = 800$ MeV ($\gamma = 1.853$) we get (see also [10])

$$\frac{\delta\bar{p}}{\bar{p}} = -\,0.18\,\frac{\delta\bar{B}}{\bar{B}} + 4.1\,\frac{\delta\bar{f}}{\bar{f}}$$

$\bar{B}$ is the average bending field and from the magnet tolerances one can estimate that it will be equal to within $\delta\bar{B}/\bar{B} = 1\ 10^{-4}$ for the four rings. $\bar{f}$ is the average revolution frequency. Before transfer the four rings will be run at equal frequencies and equal phase and a $\delta f_{acc}/f_{acc} < 5\ 10^{-6}$ can certainly be obtained. The second term will therefore at maximum be equal to the first one and in the worst case this gives a

$$\frac{\delta\bar{p}}{\bar{p}} = 4\ 10^{-5}$$

which is definitely below the resolution. Coherent synchrotron oscillations in not full buckets may however considerably increase this term.

But we have also to consider that orbit perturbations may be different in the four rings. Different closed orbit shapes imply different orbit lengths and we have to use the following equation[9], but R replaced by the orbit length C):

$$\frac{\delta\bar{p}}{\bar{p}} = \gamma^2 \frac{\delta f}{f} + \gamma^2 \frac{\delta C}{C} = 3.43 \frac{\delta f}{f} + 3.43 \frac{\delta C}{C} .$$

For Q_H half integral the influence of closed orbit distortions on the orbit length is strongest. Assuming $Q_H = 4.5$ and a maximum residual distortion $\hat{x} = 15$ mm yields a $\Delta C/C = \pm 4\ 10^{-5}$ and under these conditions a maximum of $\delta C/C = 8\ 10^{-5}$ cnn be expected.

$\delta f/f$ being small compared to that we obtain:

$$\frac{\delta\bar{p}}{\bar{p}} = 2.7\ 10^{-4}$$

about 10 times as much as can be expected from inequalities in $\bar{B}$.

Such differences can well be detected with a resolution of $(\delta\bar{p}/\bar{p})_{res} = 0.5 - 1.0\ 10^{-4}$.

Apart from detecting the effects of such extreme closed orbit conditions, the restricted spectrometer may come in useful when the Booster is not working properly and help to find the causes. And even if everything is in perfect order it is a reassuring feeling to have this confirmed by the spectrometer.

Finally one should remark, that all measurements made with the restricted spectrometer can of course be performed also with the real spectrometer, if one just adds a split-plate detector downstream of the wire detector.

DISTRIBUTION (open)

REFERENCES

1) U. Bigliani et al., Paramètres de base du système HF du synchrotron injecteur (Booster), SI/Note EL/68-2, rev. 1.

2) J.D. Jackson, Classical Electrodynamics, 1962.

3) J.F. Janni, Calculations of Energy Loss, Range, etc., US Air Force Weapons Laboratory, Technical Report AFWL-TR-65-150.

4) C. Bovet, Optique des faisceaux primaires, CERN 66-25, p. 28.

5) C. Metzger, Etude préliminaire d'un détecteur pour le spectromètre du Booster, SI/Note DL/68-18.

6) A. Ball, Private Communication.

7) C. Metzger, Spectromètre du Booster : calcul des aberrations, SI/Note DL/68-26.

8) K.L. Brown, First and Second Order Matrix Theory for the Design of Beam Transport Systems and Charged Particle Spectrometers, SLAC 75, 1967.

9) C. Bovet et al., A Selection of Formulae and Data Useful for the Design of A.G. Synchrotrons, MPS-SI/Int. DL/68-3.

10) U. Bigliani, Influence de $\Delta B/B_o$ sur les paramètres du faisceau du Booster pour le transfert du Booster au PS, MPS/Int. RF/B 67-12.

T A B L E I

All values for 800 MeV protons and degrading by 10 MeV

Material	dE/ds (MeV/cm)	Δs (mm)	$<\Delta E>$ (MeV)	$<\Delta p/p>$ (°/oo)	$<\theta>_{proj}$ (mrad)	2 Δx (mm)	$\hat{x}'$ (mrad)	F_B	P_{NI} (°/o)
Be	3.45	29.0	0.62	0.50	3.08	0.87	6.0	1.43	6.0
Mg	3.34	30.0	0.64	0.52	5.35	0.89	5.9	2.07	4.6
Al	5.01	20.0	0.64	0.52	5.58	0.72	7.2	1.84	4.6
Fe	13.34	7.5	0.66	0.54	7.88	0.44	11.8	1.67	4.2
Ni	15.21	6.6	0.67	0.54	8.23	0.42	12.6	1.64	4.2
Cu	14.54	6.9	0.67	0.54	8.38	0.42	12.3	1.69	4.2
Ag	15.60	6.4	0.68	0.55	10.69	0.41	12.8	1.95	4.0
W	24.94	4.0	0.70	0.57	13.52	0.32	16.2	1.95	3.9
Pt	27.34	3.7	0.71	0.57	13.91	0.31	16.9	1.92	3.8
Pb	14.21	7.0	0.71	0.58	14.28	0.43	12.2	2.55	3.8

dE/ds	specific energy loss
Δs	thickness of slit jaws for degrading by 10 MeV
$<\Delta E>$	rms-value of energy straggling
$<\Delta p/p>$	rms-value of momentum straggling
$<\theta>_{proj}$	rms-value of projected scattering angle
2 Δx	permitted total slit width
$\hat{x}'$	resulting maximum divergence at the slit for ε_s = 2.62 mm mrad
F_B	emittance blow-up of total beam
P_{NI}	probability for inelastic nuclear interactions.

T A B L E I

All values for 800 MeV protons and degrading by 10 MeV

Material	dE/ds (MeV/cm)	Δs (mm)	$<\Delta E>$ (MeV)	$<\Delta p/p>$ (°/oo)	$<\theta>_{proj}$ (mrad)	2 Δx (mm)	$\hat{x}'$ (mrad)	F_B	P_{NI} (°/o)
Be	3.45	29.0	0.62	0.50	3.08	0.87	6.0	1.43	6.0
Mg	3.34	30.0	0.64	0.52	5.35	0.89	5.9	2.07	4.6
Al	5.01	20.0	0.64	0.52	5.58	0.72	7.2	1.84	4.6
Fe	13.34	7.5	0.66	0.54	7.88	0.44	11.8	1.67	4.2
Ni	15.21	6.6	0.67	0.54	8.23	0.42	12.6	1.64	4.2
Cu	14.54	6.9	0.67	0.54	8.38	0.42	12.3	1.69	4.2
Ag	15.60	6.4	0.68	0.55	10.69	0.41	12.8	1.95	4.0
W	24.94	4.0	0.70	0.57	13.52	0.32	16.2	1.95	3.9
Pt	27.34	3.7	0.71	0.57	13.91	0.31	16.9	1.92	3.8
Pb	14.21	7.0	0.71	0.58	14.28	0.43	12.2	2.55	3.8

dE/ds	specific energy loss
Δs	thickness of slit jaws for degrading by 10 MeV
$<\Delta E>$	rms-value of energy straggling
$<\Delta p/p>$	rms-value of momentum straggling
$<\theta>_{proj}$	rms-value of projected scattering angle
2 Δx	permitted total slit width
$\hat{x}'$	resulting maximum divergence at the slit for ε_s = 2.62 mm mrad
F_B	emittance blow-up of total beam
P_{NI}	probability for inelastic nuclear interactions.

T A B L E II

Real Spectrometer

Element	Dimensions	Configuration	Power Supply (kW)	Price in kFr	
				element	supply
quadrupole Q_{s1}	as standard transfer	as standard transfer	10	15	30
quadrupole Q_{s2}	"	"	10	15	30
quadrupole Q_{s4}	r = 0.16m g = 750G/cm ℓ = 0.80m $\hat{B}$ = 10kG	high precision end shaping mirror plates	50	60	60
quadrupole Q_{s5}	"	"	50	60	60
quadrupole Q_{s6}	"	"	50	60	60
bending magnet + 9°	ℓ = 0.65m B = 15kG free aperture: hor.: 0.40m vert.: 0.10m	rectangular window frame standard precision	100	60	60
bending magnet - 30°	ℓ = 2.56m B = 10kG free aperture: hor.: 0.40m vert.: 0.15m	sector, C-type high precision, end shaping, mirror plates	300	220	80
				490	380

Total 870

TABLE III

Restricted Spectrometer

Element	Dimensions	Configuration	Power Supply (kW)	Price in kFr	
				element	supply
quadrupole Q_{s2}	as standard transfer	as standard transfer	10	15	30
quadrupole Q_{s3}	"	"	10	15	30
quadrupole Q_{s4}	"	"	10	15	30
bending magnet $\pm 10^{o}$	ℓ = 0.65m B = 15kG free aperture: hor.: 0.24m vert.:0.08m	rectangular window frame standard precision	100	50	60
bending magnet -16^{o}	ℓ = 1.00m B = 15kG free aperture: hor.: 0.18m vert.:0.08m	rectangular window frame standard precision	100	60	60
				155	210
			Total	365	

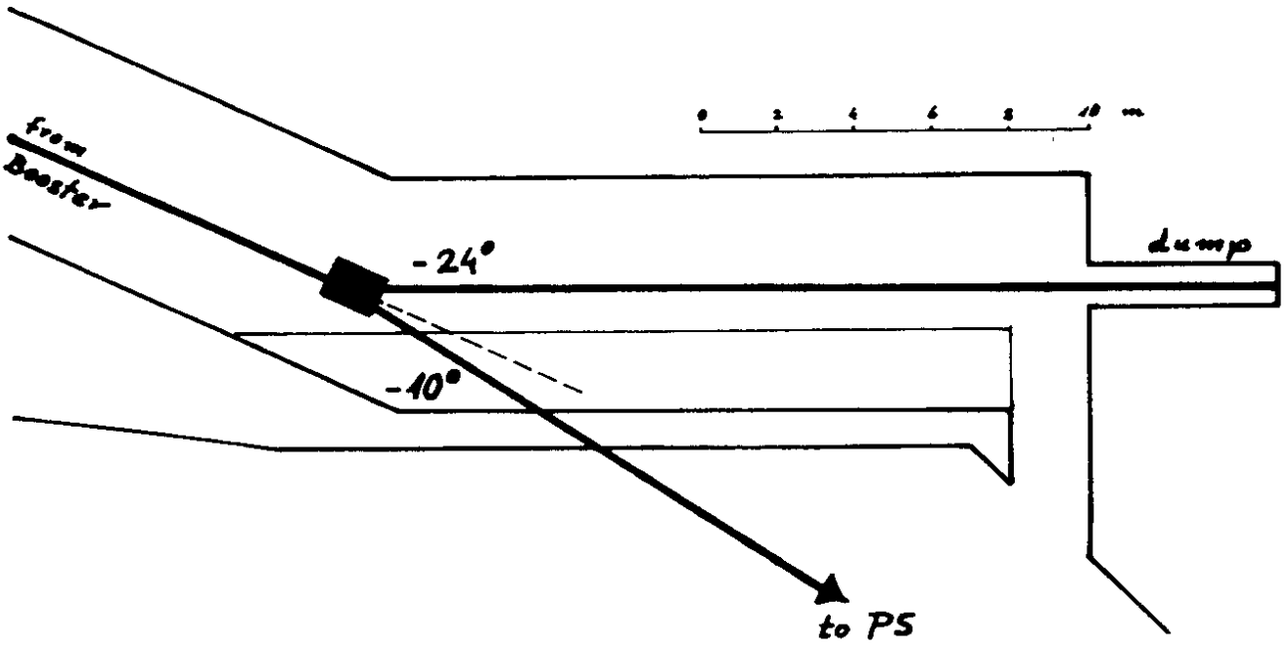

FIG. 1

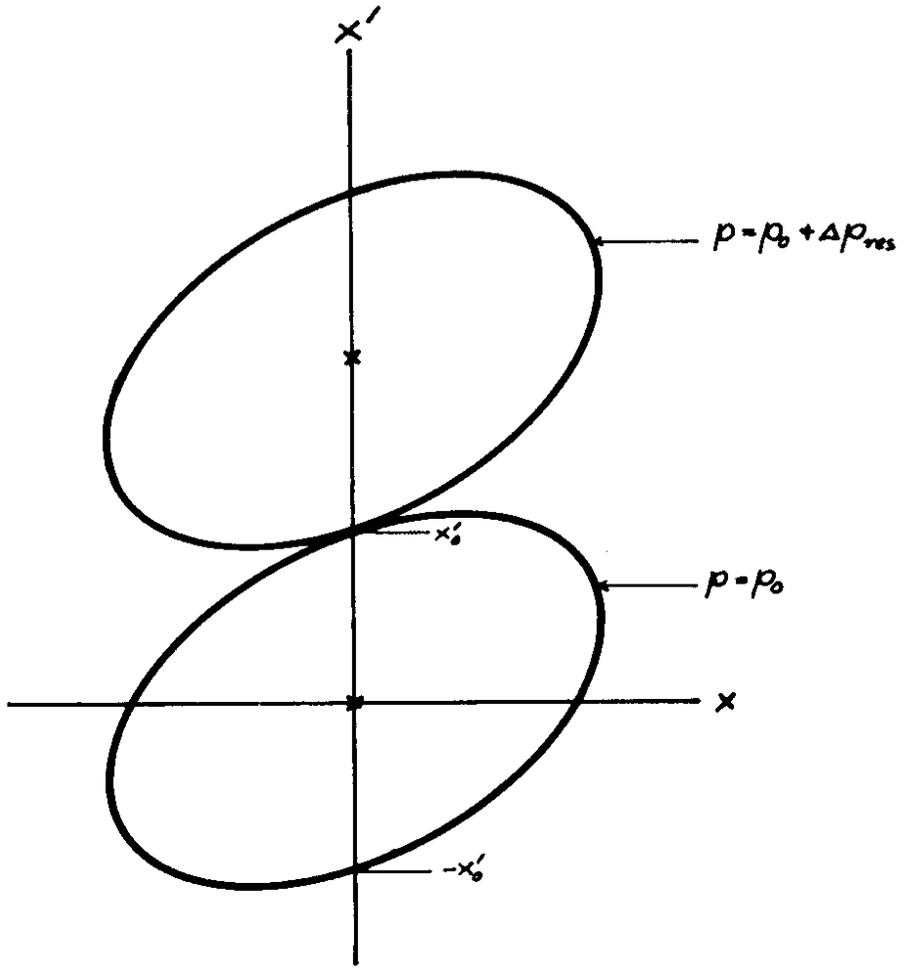

FIG. 2

H.K.12.68

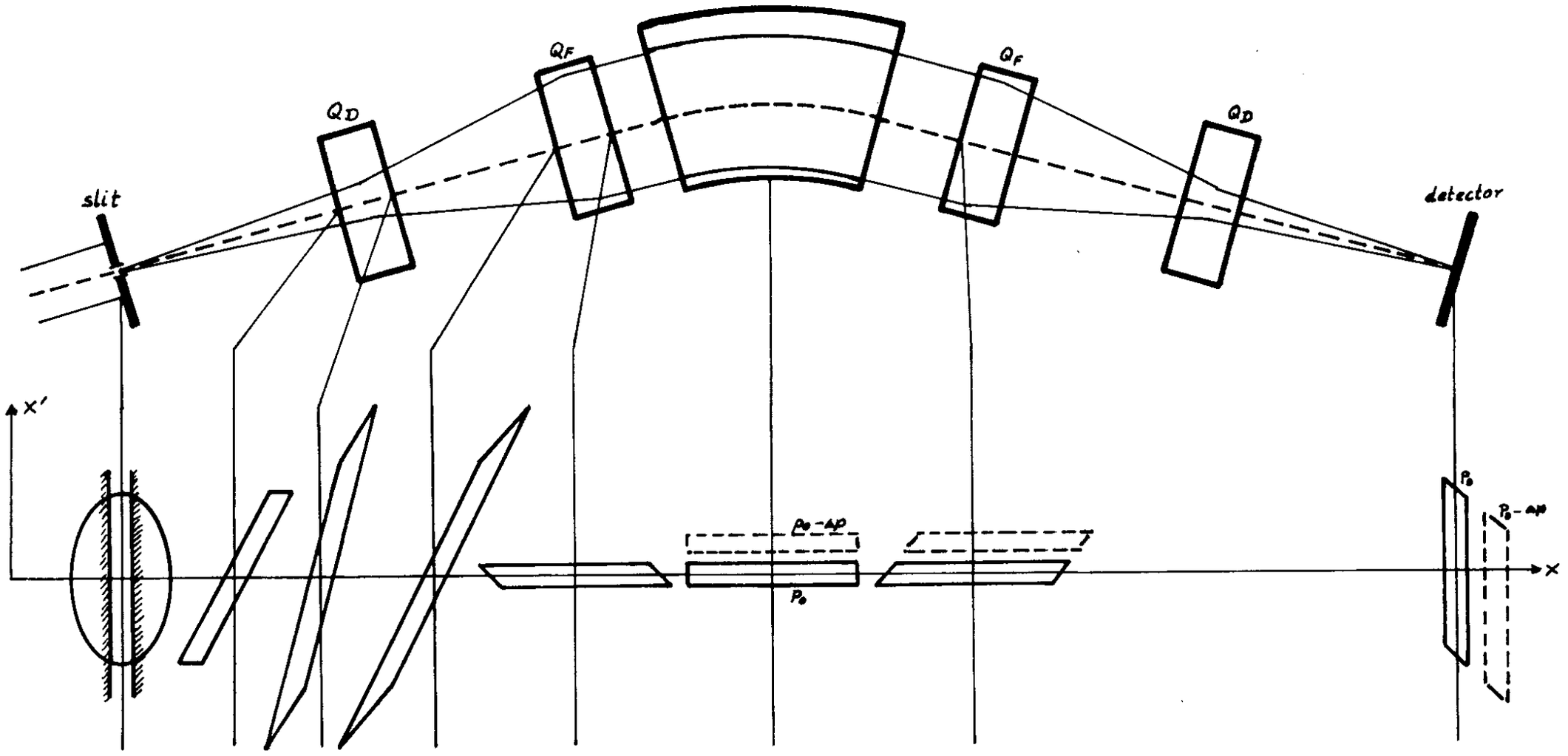

FIG. 3

H.K.12.68.

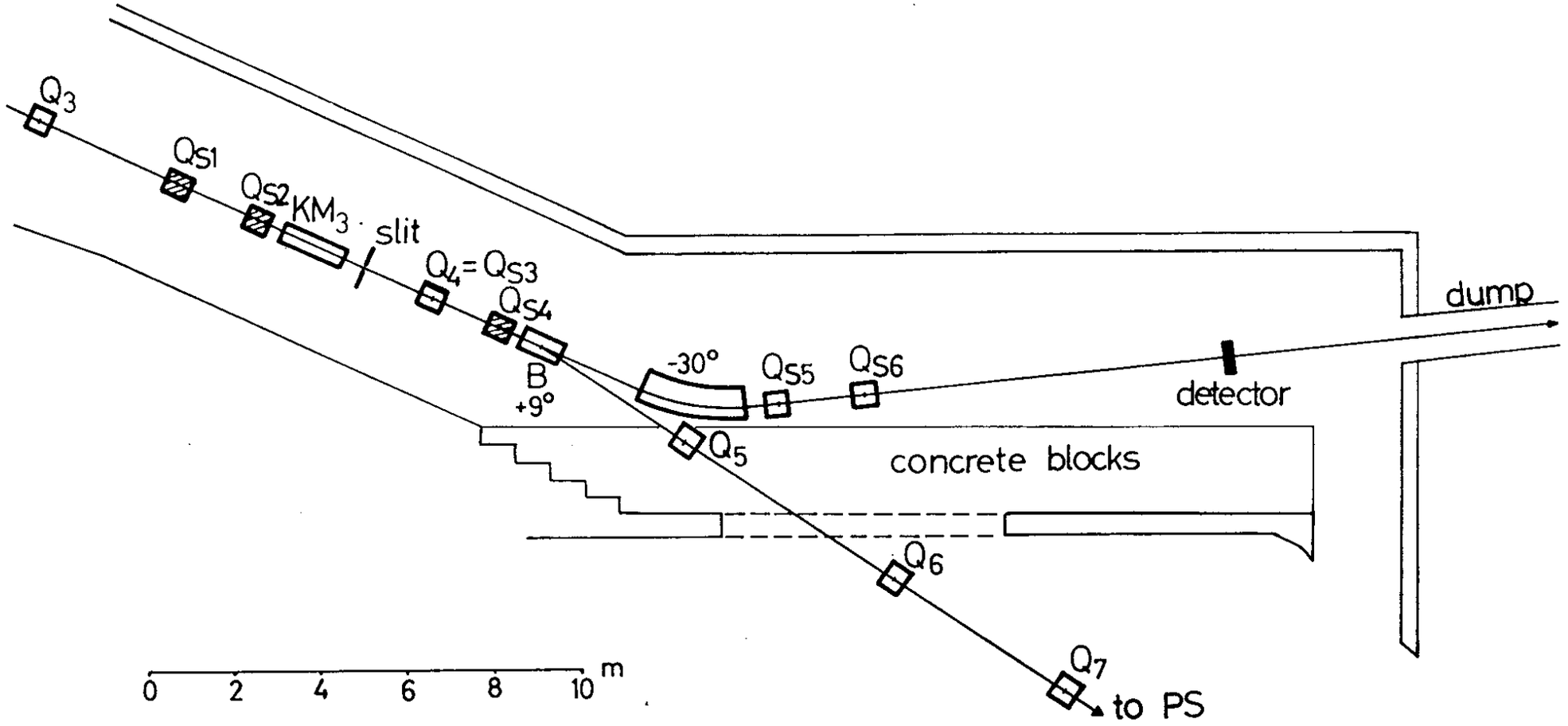

real spectrometer

FIG. 4

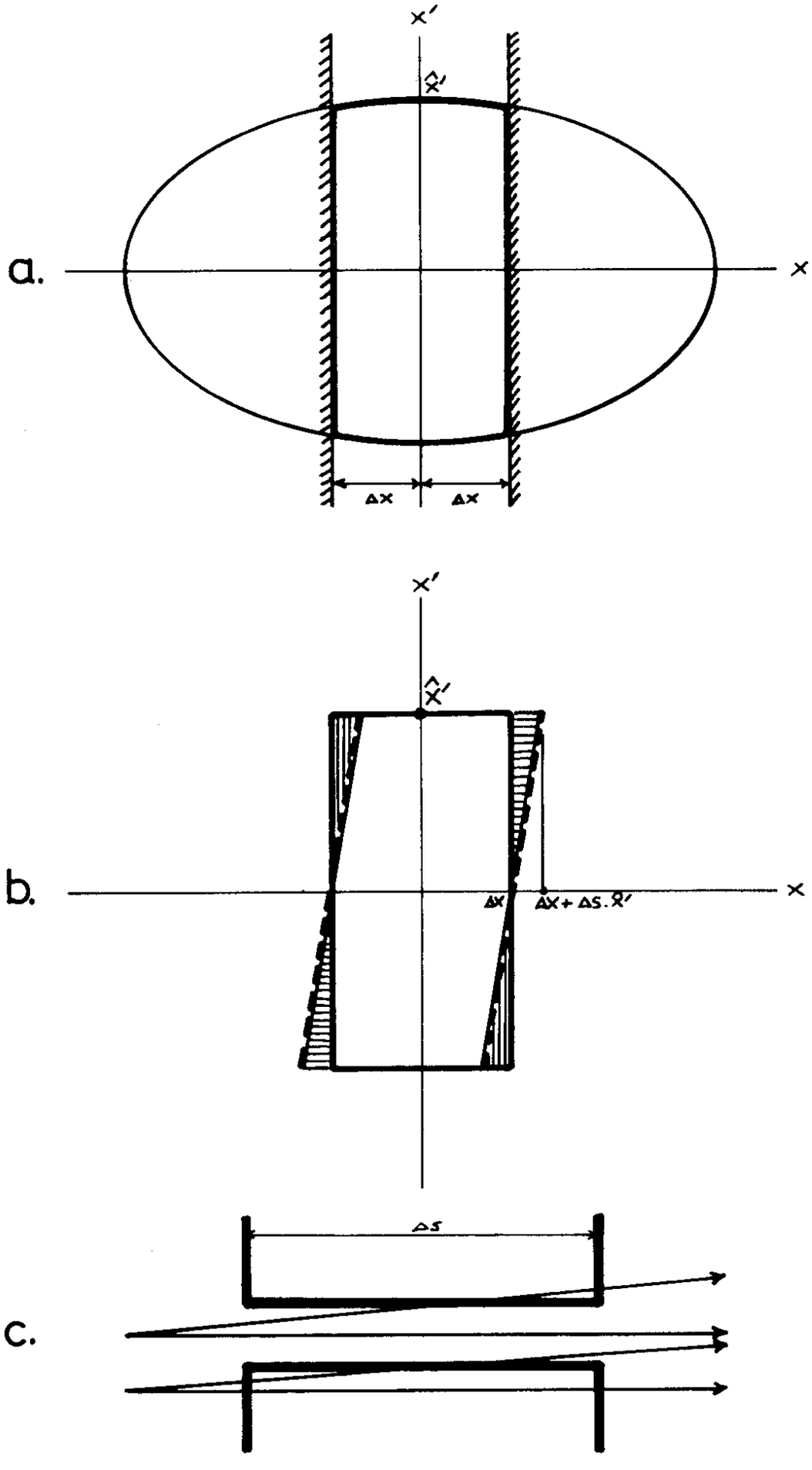

FIG. 5

H.K.12.68.

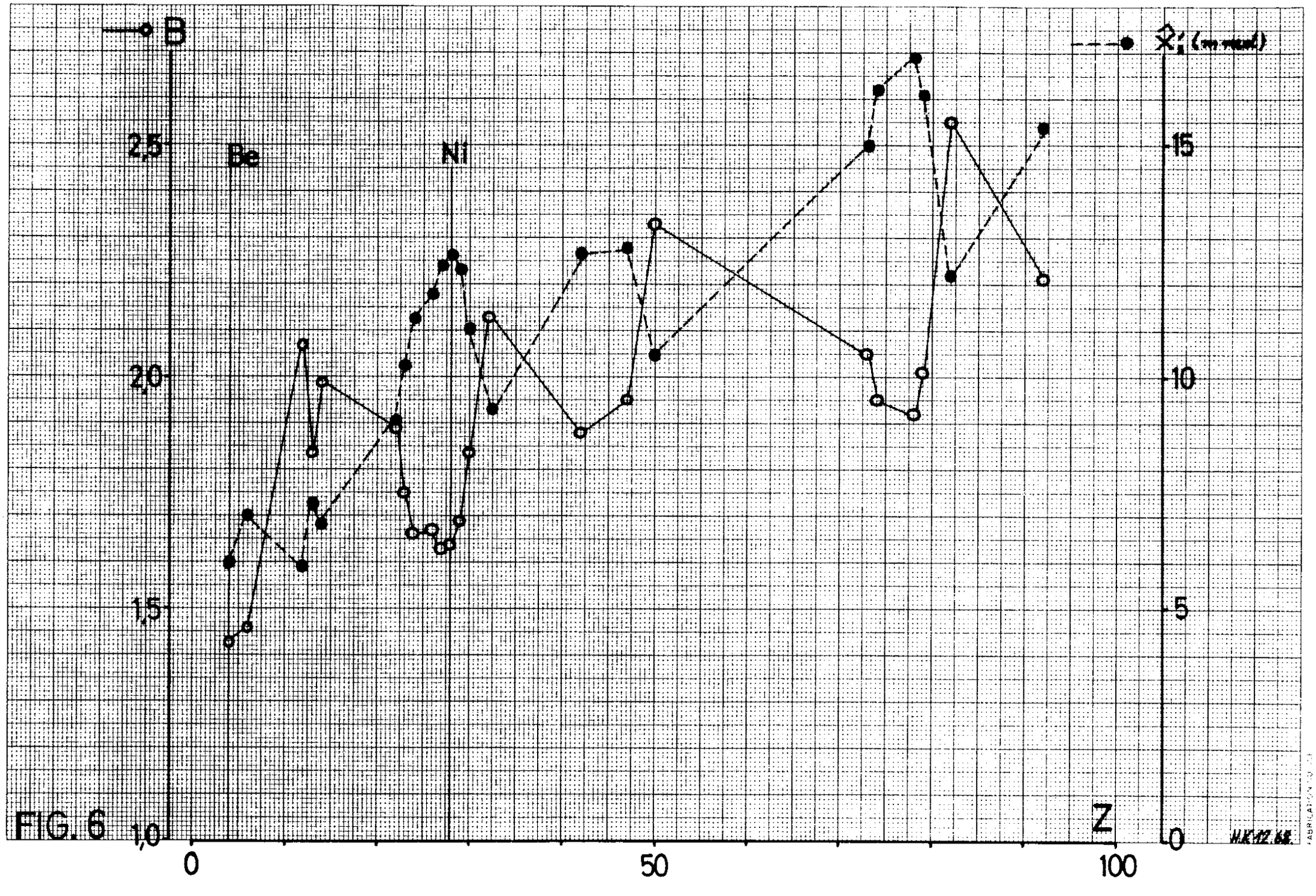

FIG. 6

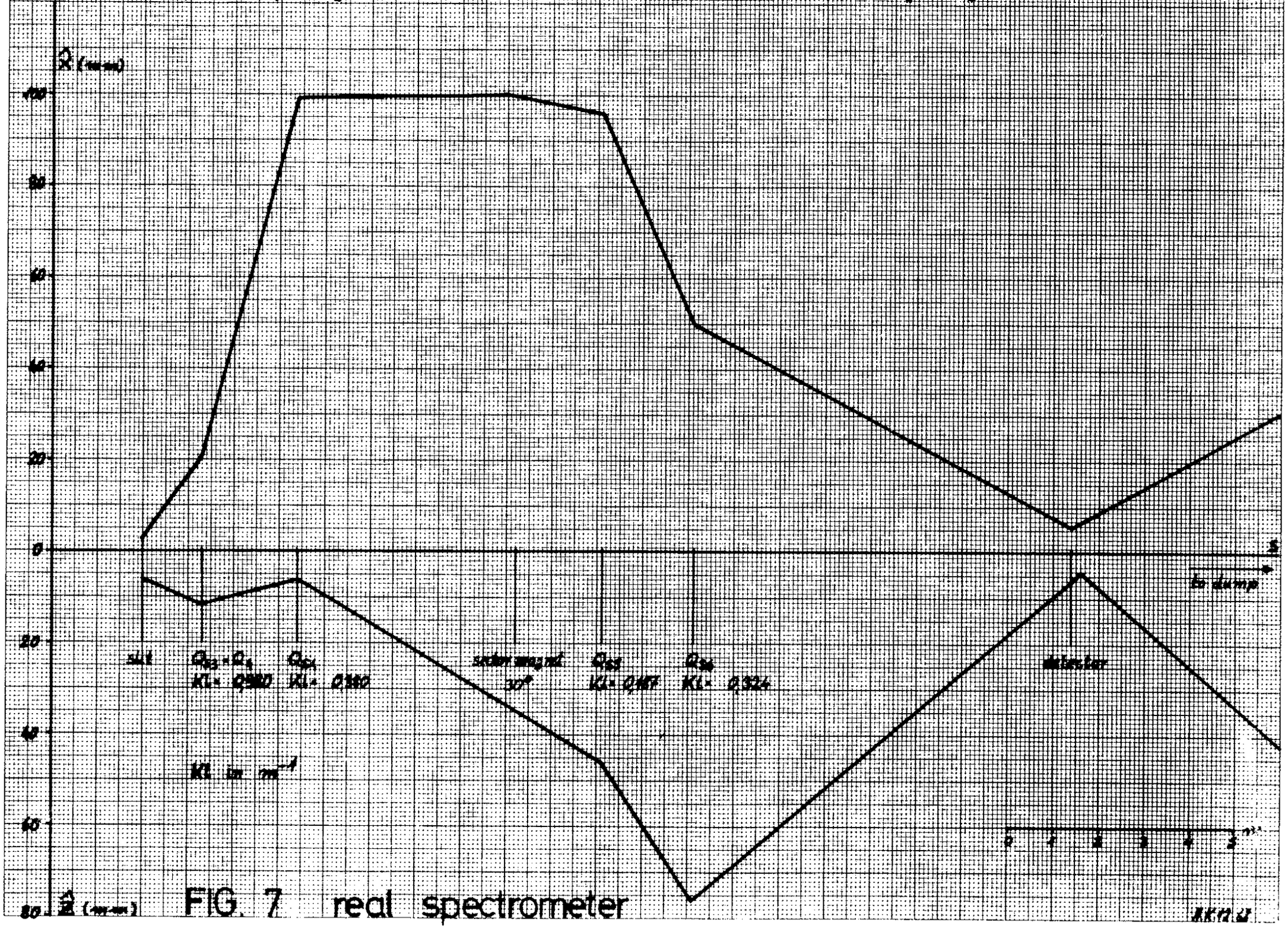

FIG. 7 real spectrometer

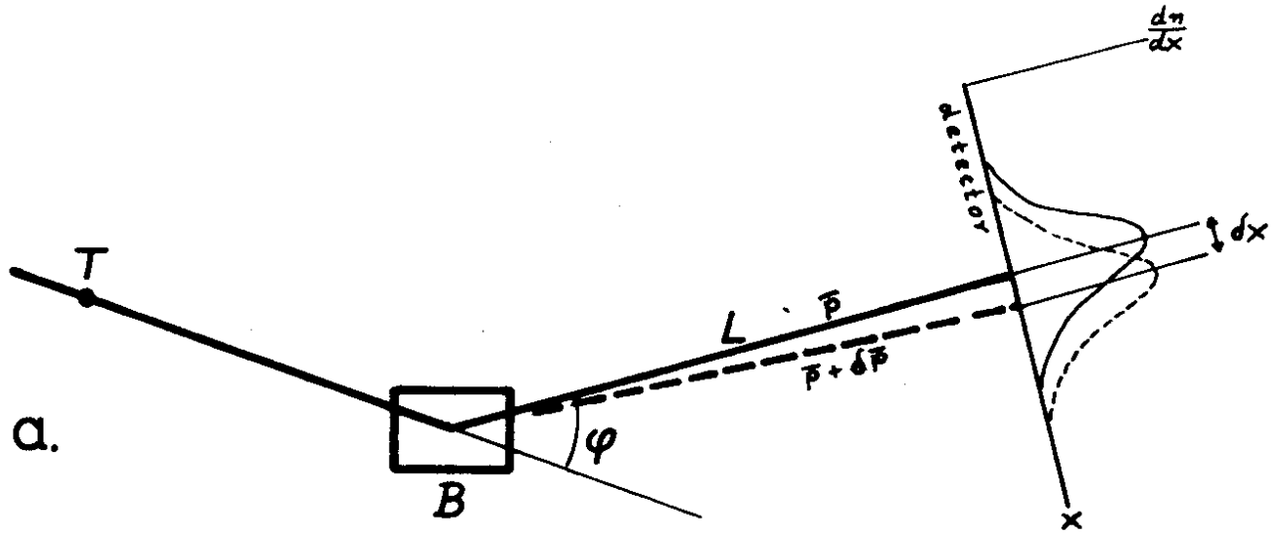

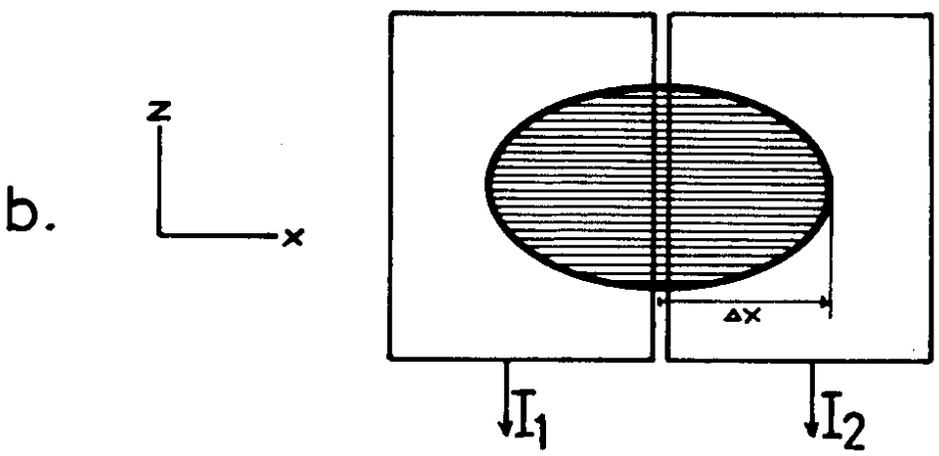

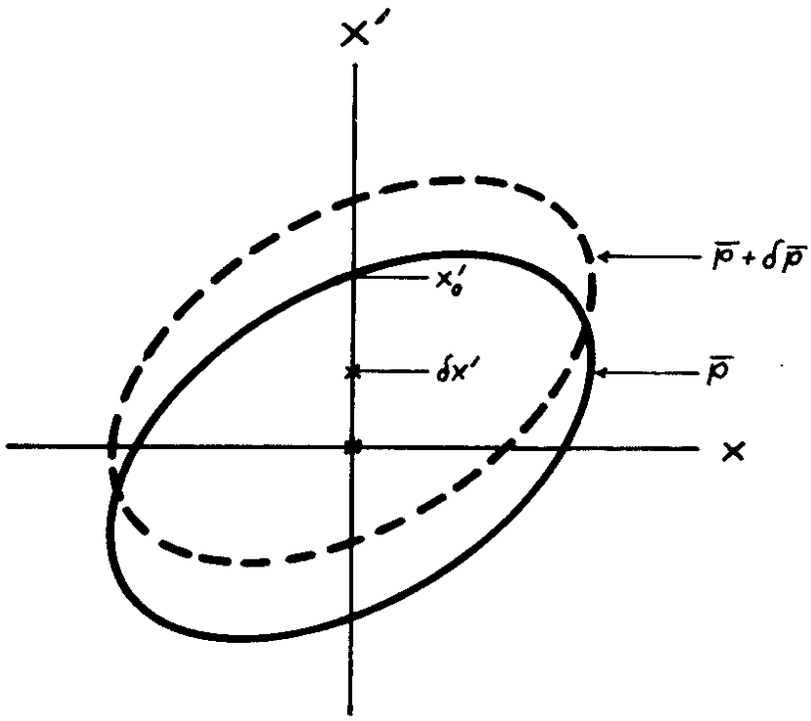

FIG. 8

H.K.12.68.

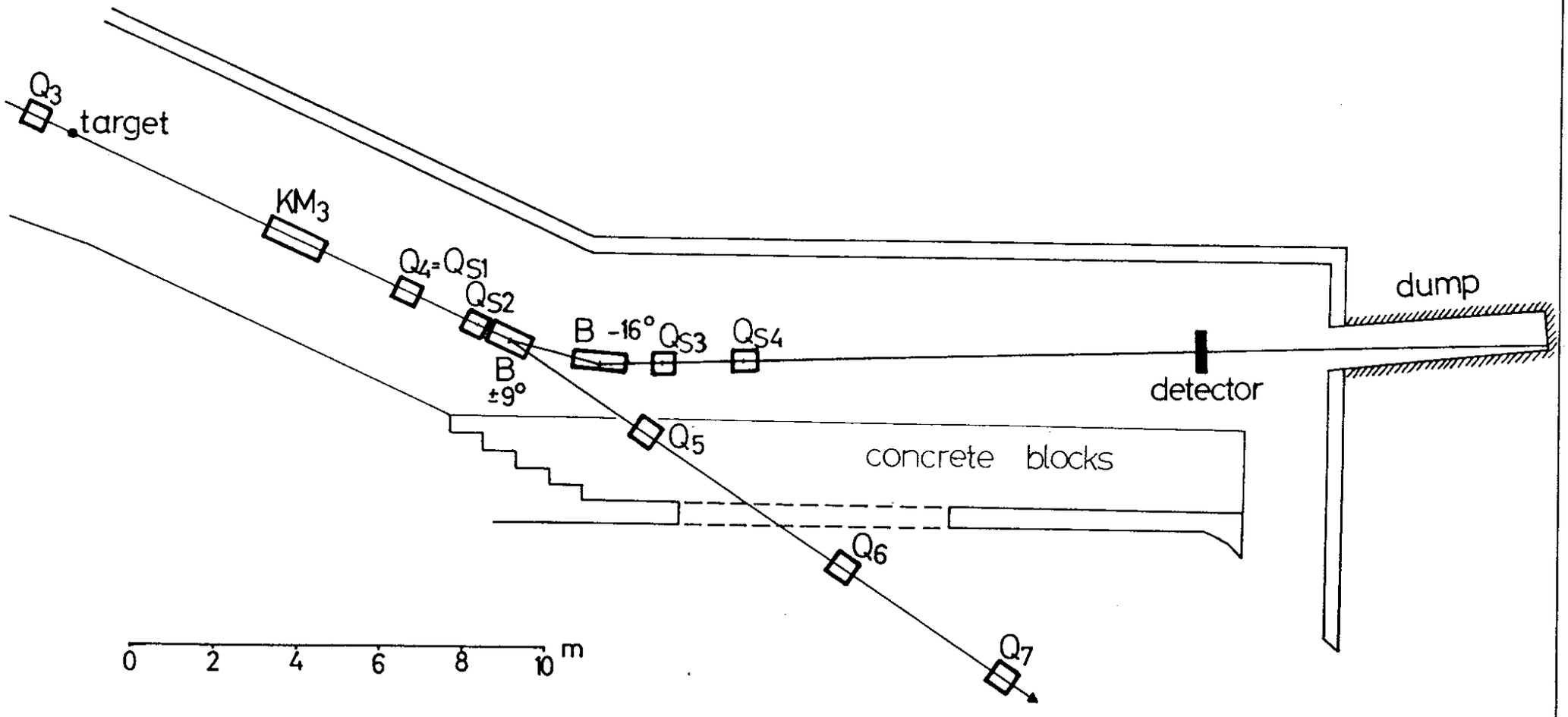

restricted spectrometer

FIG. 9

H.K.12.68

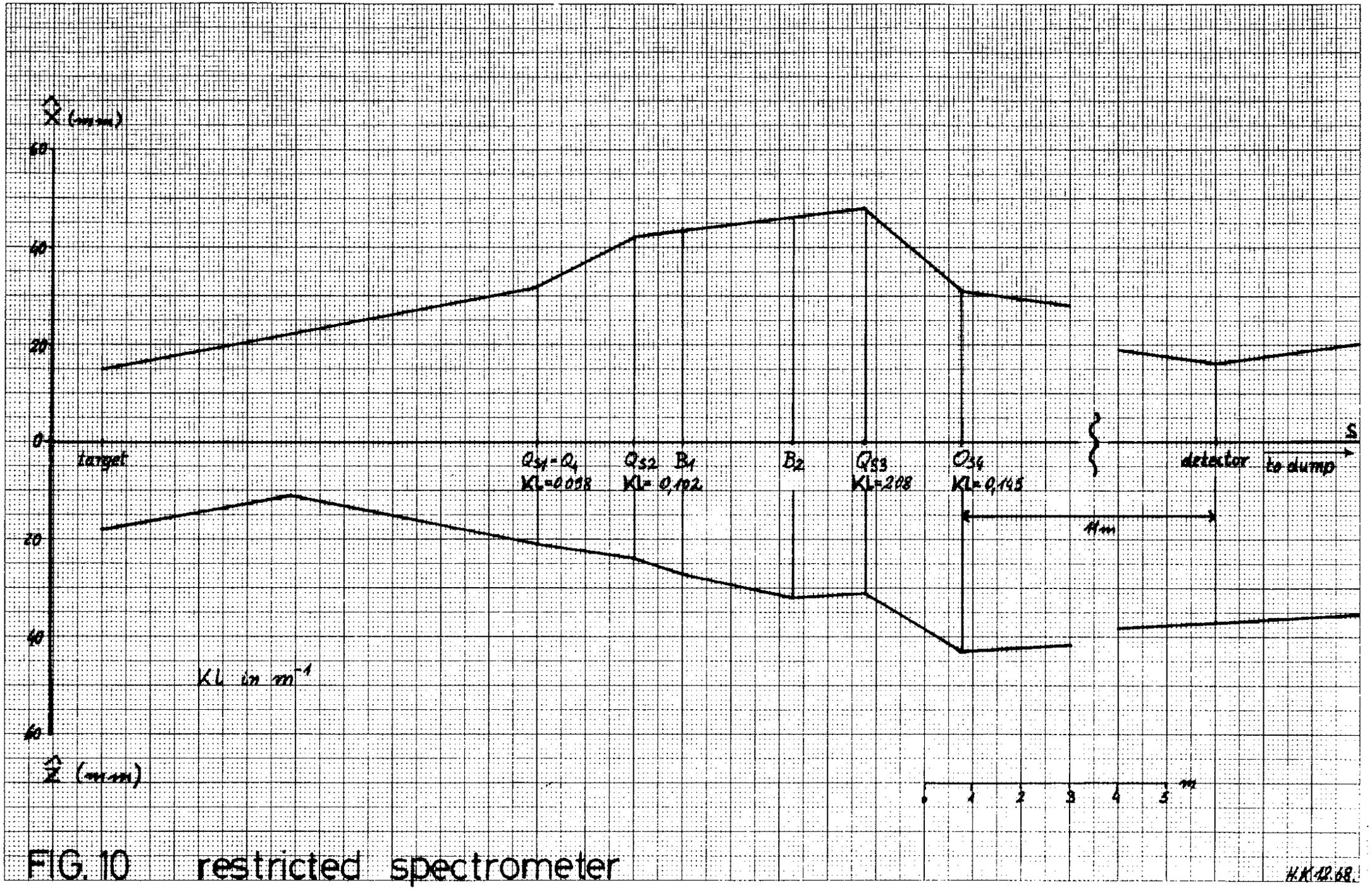

FIG. 10 restricted spectrometer

H.K 12.68.

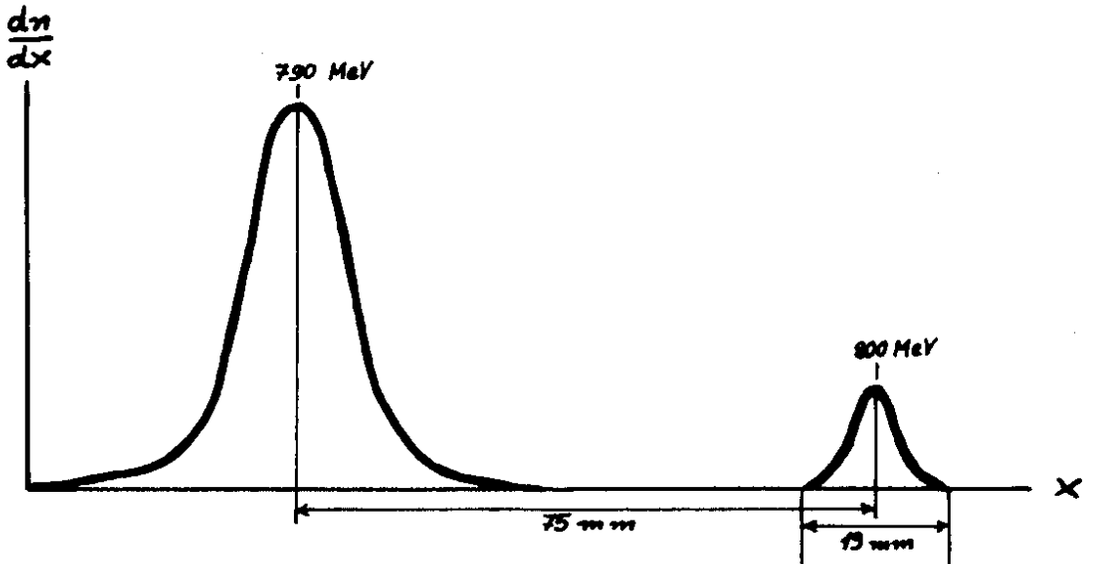

a. real spectrometer

situation at the detector

b. restricted spectrometer

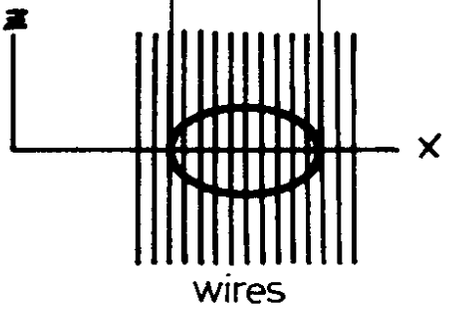

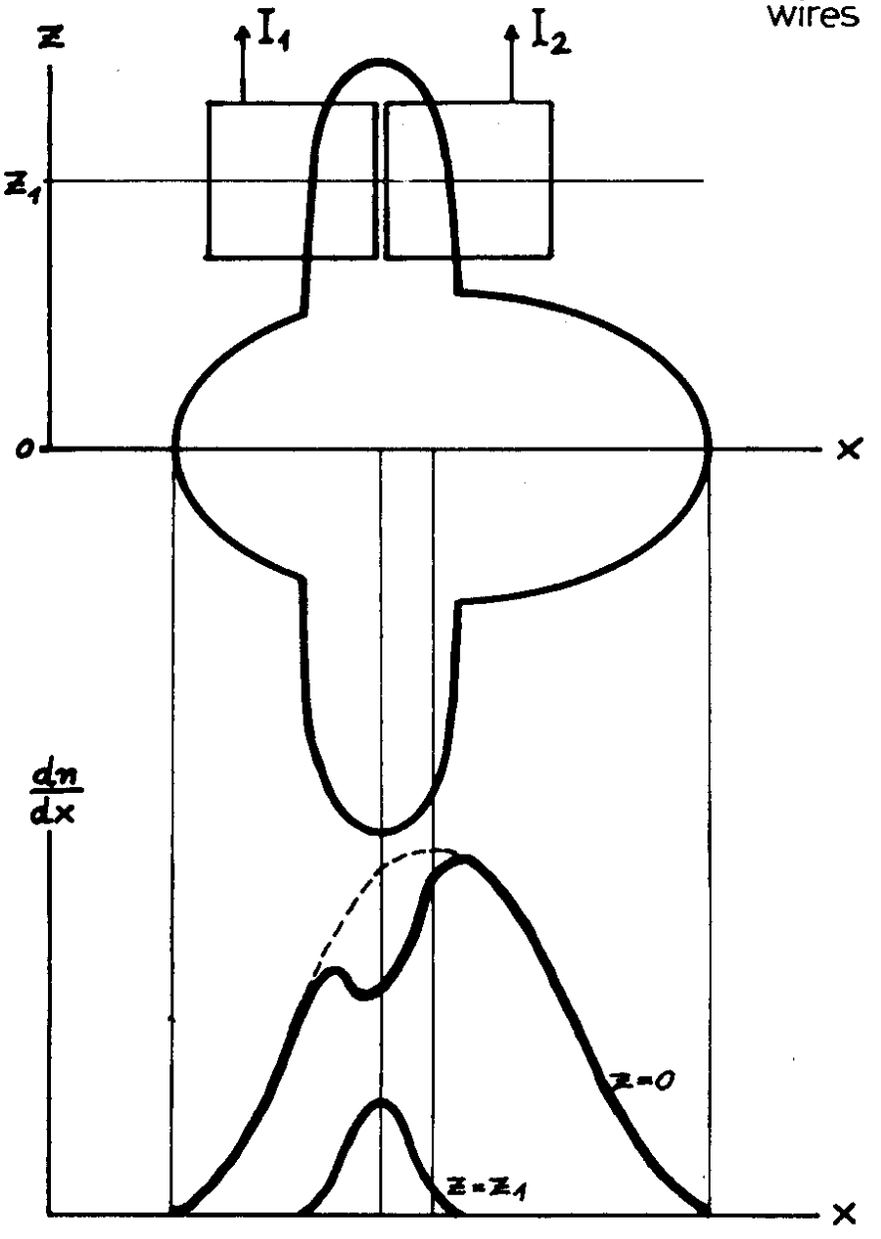

FIG. 11

H.K.12.68.